Inhomogenous Electronic Structure, Transport Gap, and Percolation Threshold in Disordered Bilayer Graphene

E. Rossi[1] and S. Das Sarma[2]

[1]*Department of Physics, College of William and Mary, Williamsburg, Virginia 23187, USA*
[2]*Condensed Matter Theory Center, Department of Physics, University of Maryland, College Park, Maryland 20742-4111, USA*
(Received 18 March 2011; published 5 October 2011)

The inhomogenous real-space electronic structure of gapless and gapped disordered bilayer graphene is calculated in the presence of quenched charge impurities. For gapped bilayer graphene, we find that for current experimental conditions the amplitude of the fluctuations of the screened disorder potential is of the order of (or often larger than) the intrinsic gap Δ induced by the application of a perpendicular electric field. We calculate the crossover chemical potential Δ_{cr}, separating the insulating regime from a percolative regime in which less than half of the area of the bilayer graphene sample is insulating. We find that most of the current experiments are in the percolative regime with $\Delta_{cr} \ll \Delta$. The huge suppression of Δ_{cr} compared with Δ provides a possible explanation for the large difference between the theoretical band gap Δ and the experimentally extracted transport gap.

One of the unique properties of single layer graphene (SLG) [1] is its high room-temperature electronic mobility [2]. This fact makes graphene of great interest for possible technological applications. However, the lack of a band gap implies that in SLG the current can never be turned off completely (i.e., SLG has a very low on-off ratio in the engineering jargon) and therefore limits the possible use of SLG in transistor or switching applications. The mobility of bilayer graphene (BLG) is normally lower than the mobility of SLG [3–5], but it can be very high when boron nitride is used as a substrate [6,7]. Most importantly, by applying a perpendicular electric field [8–14], a gap of up to 250 meV can be opened in the band structure of BLG which should strongly enhance the on-off switching ratio. The strictly 2D nature of the carriers, the high room-temperature mobility, and the ability to open and tune Δ make BLG an extremely interesting material from both a fundamental and a technological point of view. In recent BLG experiments [11–13], the activated transport gap has been found to be orders of magnitude smaller than Δ. This finding has been explained by assuming that transport is in the variable range hopping regime [11–13] or that edge modes might contribute significantly to transport [15]. Resonant scattering centers have been proposed as the dominant source of disorder [16] in both SLG and BLG. In gapped BLG the resonant scatterers would induce localized states that would then mediate transport via variable range hopping. However, scanning tunneling microscopy experiments have so far not shown direct evidence of resonant states suggesting that their density might be quite low; in addition, no sign of localization is ever observed in ungapped BLG even in the presence of strong disorder. On the other hand, the edge modes can significantly contribute only if scattering between counterpropagating edge modes is suppressed. Because the BLG band

structure is characterized by two equivalent valleys with opposite chirality, even small quantities of short-range defects can mix the fermionic states of the two valleys and greatly suppress the contribution of the edge modes to transport [14]. These facts motivated us to look for a possible alternative explanation to the smallness of the experimental BLG transport gap compared to Δ based on the disorder-induced massive breakdown of momentum conservation.

Our model is based on the assumption that charge impurities are the dominant source of disorder in exfoliated BLG samples. There is ample evidence [2] that this assumption is at least consistent with most of the transport experiments on gapless SLG and BLG, although other scattering sources might play an important role [16,17]. In particular, we assume the charge impurities to be located at a typical distance $d \approx 1$ nm from the graphenic layer and to be uncorrelated. In reality, some degree of correlation is expected, but it does not affect qualitatively our results. In the presence of charge impurities, the carrier density becomes strongly inhomogenous. The importance of density inhomogeneities for the understanding of the physics, especially transport, of 2D electronic systems has been appreciated in the context of the quantum Hall effect [18] and of *standard* 2D electron gases (2DEGs), in which the gap between the hole band and the electron band is much larger than the disorder strength [19]. The case of gapped BLG is different from these cases, because no magnetic field is present and so the dispersion is not broken up in Landau levels, and yet the band gap is small compared to the strength of the disorder potential. We emphasize, moreover, that the transport phase diagram, which is the main topic of our work, has never before been addressed in the literature for any system. In BLG we therefore have the unique condition of a small band gap between

nondegenerate valence and conduction bands. The most striking and counterintuitive consequence of this fact is that, as we show below, in gapped BLG an *increase* of the disorder strength can drive the system from being an insulator to being a bad metal when the chemical potential μ is within the gap. This behavior is the opposite of what happens in a standard 2DEG, in which an increase of the disorder strength drives the system to an insulating state. By showing that the disorder can effectively drive BLG to a metal state even when Δ is finite and μ is well within the gap, our work provides a compelling possible explanation for the large discrepancy between Δ of gapped BLG and the gap extracted from transport measurements. We define an effective *real-space* gap Δ_{cr} that determines the transport properties and show that for disorder strengths typical in current experiments it can be zero even for Δ as large as 150 meV. Although our specific calculations are carried out for gapped BLG systems, the general idea developed here, namely, a spatially fluctuating local band gap in the presence of charged impurity disorder-induced inhomogeneity, should apply to other systems, and we believe that the same idea could explain the experimental finding [20] of rather small transport band gaps in graphene nanoribbon experiments where percolation effects are known to be important.

Our main goal is to find a qualitative explanation for the smallness of the transport gap compared to Δ for the situation when charge impurities are the dominant source of disorder. To calculate the electronic structure in the presence of the disorder potential due to charge impurities, we use the Thomas-Fermi theory (TFT). For SLG the TFT results [21] compare well with density functional theory results [22] and experiments [23–25] as long as the impurity density n_{imp} is not too low ($\gtrsim 10^{11}$ cm^{-2}) [26]. These results suggest that the TFT might give reasonable results also for disordered BLG. The TFT is valid when the density profile $n(\mathbf{r})$ satisfies the inequality $|\nabla n / n| < k_F$, with $k_F = \sqrt{\pi n}$ the Fermi wave vector. As shown below, the density varies on length scales of the order of 10–20 nm, whereas in the metallic regions $n \approx 2 \times 10^{12}$ cm^{-2}, so that the inequality $|\nabla n / n| < k_F$ is only marginally satisfied. A complete quantitative validation of the TFT results can be achieved only by comparison to density functional theory results that, however, are not yet available for disordered BLG. On the other hand, due to the computational cost, density functional theory cannot be used to calculate disorder-averaged quantities that are needed to extract the transport properties. The TFT is therefore the only approach that can be used to address the issue of transport in BLG in the presence of long range disorder and, given that our goal is the *qualitative* understanding of the large difference between transport gap and Δ, is also adequate. Moreover, the strong dependence of the transport gap on the details of the experiments (like the temperature range) makes a quantitative comparison of theory and experiments almost impossible. For this reason,

and given the limited quantitative accuracy of the TFT, for the band structure of BLG we use the simple model of 2 parabolic bands with effective mass $m^* = 0.033 m_e$. The simplicity of this model allows us to identify the few parameters that affect the qualitative features of the results and makes our findings relevant also to standard parabolic 2DEGs.

The TFT energy functional is given by

$$E[n] = \int d\mathbf{r} \left(\frac{\pi \hbar^2}{4 m^*} n^2 + \frac{\Delta}{2} |n| \right) + \frac{e^2}{2\epsilon} \int d\mathbf{r}' \int d\mathbf{r} \frac{n(\mathbf{r}) n(\mathbf{r}')}{|\mathbf{r} - \mathbf{r}'|}$$
$$+ \frac{e^2}{\epsilon} \int d\mathbf{r} V_D(\mathbf{r}) n(\mathbf{r}) - \mu \int d\mathbf{r} n(\mathbf{r}), \quad (1)$$

where ϵ is the static background dielectric constant and $e V_D / \epsilon$ the bare disorder potential. The first term is the kinetic energy, the second is the Hartree part of the Coulomb interaction, and the third is the contribution due to the disorder potential. Assuming $\epsilon = 4$ for the substrate, as appropriate for graphene on SiO$_2$, in the remainder we set $\epsilon = 2.5$, the average of the dielectric constant of the vacuum and substrate. By differentiating $E[n]$ with respect to n, we find

$$\frac{2m^*}{\hbar^2} \frac{\delta E}{\delta n} = \pi n + \frac{m^* \Delta}{\hbar^2} \text{sgn}(n) + \frac{1}{2 r_{sc}} \int \frac{n(\mathbf{r}') d\mathbf{r}'}{|\mathbf{r} - \mathbf{r}'|}$$
$$+ \frac{V_D(\mathbf{r})}{r_{sc}} - \frac{2m^* \mu}{\hbar^2}, \quad (2)$$

where we have introduced the *screening length* $r_{sc} \equiv [(2e^2 m^*)/(\epsilon \hbar^2)]^{-1} \approx 2$ nm.

At the energy minimum, $\delta E / \delta n = 0$. For the gapless case this equation can be solved analytically in momentum space to find

$$n(\mathbf{q}) = -\frac{V_D(\mathbf{q})}{\pi r_{sc}} \frac{q}{q + r_{sc}^{-1}}. \quad (3)$$

Let $\hat{V}_{D,sc}(\mathbf{r}) = r_{sc}^{-1} V_D(\mathbf{r}) + (1/2 r_{sc}) \int d\mathbf{r}' n(\mathbf{r}')/|\mathbf{r} - \mathbf{r}'|$ be the screened disorder potential. Using Eq. (3), we find

$$\hat{V}_{D,sc}(\mathbf{q}) = \frac{V_D(\mathbf{q})}{r_{sc}} \frac{q}{q + r_{sc}^{-1}} = -\pi n(q). \quad (4)$$

We have $V_D(\mathbf{q}) = A(\mathbf{q}) e^{-qd}/q$, where $A(\mathbf{q})$ are random numbers with Gaussian distribution such that $\langle A \rangle = 0$ and $\langle A^2 \rangle = n_{imp}$, where the angle brackets denote the average over disorder realizations. Using Eqs. (3) and (4) and the statistical properties of $A(\mathbf{q})$, for the variance of the density $\text{Var}(n)$, we find

$$\text{Var}(n) = \frac{2 n_{imp}}{\pi r_{sc}^2} \int_0^\infty dq \frac{q e^{-2qd}}{(q + r_{sc}^{-1})^2} = \frac{2 n_{imp}}{\pi r_{sc}^2} f(d/r_{sc}) \quad (5)$$

with $f(d/r_{sc}) = e^{2d/r_{sc}}(1 + 2d/r_{sc}) \Gamma(0, 2d/r_{sc}) - 1$, a dimensionless function [here $\Gamma(a, x)$ is the incomplete gamma function]. For small d/r_{sc}, $f = -1 - \gamma - \log(2d/r_{sc}) + O(d/r_{sc})$ (where $\gamma = 0.577216$ is the Euler

constant), whereas for $d \gg r_{sc}$ $f = 1/(2d/r_{sc})^2 + O((d/r_{sc})^{-3})$. For the root mean square of the density, $n^{(rms)}$, and screened disorder potential $V_{D,sc}^{(rms)} = (\hbar^2/2m^*)\hat{V}_{D,sc}^{(rms)}$, we then have, respectively,

$$n^{(rms)} = \frac{\sqrt{n_{imp}}}{r_{sc}}\left[\frac{2}{\pi}f(d/r_{sc})\right]^{1/2}, \quad V_{D,sc}^{(rms)} = \frac{\hbar^2\pi}{2m^*}n^{(rms)}. \quad (6)$$

In the presence of a band gap, the equation $\delta E/\delta n = 0$ becomes nonlinear and an analytic expression for $n^{(rms)}$ is not readily obtainable. We have solved the problem numerically for 100×100 nm samples, with 1 nm spatial discretization, considering several (1000 or more) disorder realizations to then calculate the disorder-averaged quantities. In Figs. 1(a) and 1(b), we show our calculated carrier density landscapes for single disorder realizations for two values of Δ, both with the same n_{imp} and μ fixed at the charge neutrality point (CNP). In the absence of disorder, both situations in Figs. 1(a) and 1(b) will manifest zero carrier density throughout with a pure intrinsic band gap at all spatial points (i.e., both sets of plots will be completely "white" in color since we are explicitly at $T = 0$ with no thermal interband excitations). Figures 1(c) and 1(d) show the dependence of $n^{(rms)}$ and $V_{D,sc}^{(rms)}$, respectively, on the doping n for values of the gap between 12 and 55 meV. $n^{(rms)}$ is suppressed close to the CNP, due to the large area covered by insulating regions
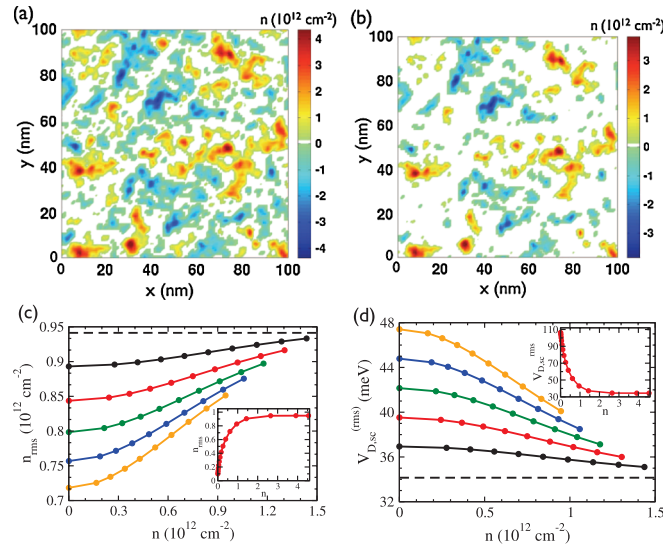
($n = 0$), whereas $V_{D,sc}^{(rms)}$ is higher close to the CNP due to the lack of screening. The results of Figs. 1(c) and 1(d) are well fitted by the scalings $n^{(rms)} = n^{(rms)}(\Delta = 0) - 9 \times 10^{-3}\Delta^{0.78}e^{-n^2/b_n}$, $V_{D,sc}^{(rms)} = V_{D,sc}^{(rms)}(\Delta = 0) + 0.24\Delta e^{-n^2/b_v}$, with $b_n = 1.83e^{-\Delta/98.5}$, $b_v = 2.31e^{-\Delta/73.26}$, and n and Δ expressed in units of 10^{12} cm^{-2} and meV, respectively.

The analysis of the disorder-averaged results obtained from the TFT can be used to qualitatively understand the electronic transport in the highly inhomogenous density landscape of gapped BLG. Let A_i be the disorder-averaged fraction of the area occupied by the insulating regions [white in Figs. 1(a) and 1(b)]. The color plots in Figs. 2(a)–2(c) show the dependence of A_i on n_{imp} and the doping $\langle n \rangle$ for three different values of Δ. At high dopings and low disorder, A_i is fairly small. As $\langle n \rangle$ decreases, some hole puddles and insulating regions start appearing. The black line identifies the contour for which $n^{(rms)} = \langle n \rangle$. Below the black line, $n^{(rms)} > \langle n \rangle$, and we are in the strongly inhomogenous regime. The white line identifies
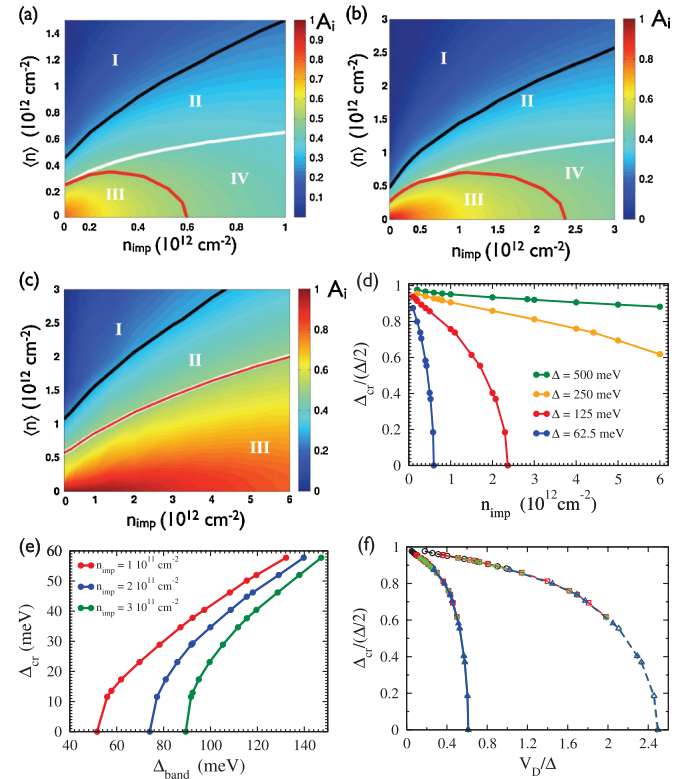

FIG. 1 (color online). Color plot of $n(\mathbf{r})$ at the CNP for a single disorder realization in gapped BLG, for $n_{imp} = 8 \times 10^{11}$ cm^{-2}, $d = 1$ nm, and $\Delta = 125$ meV (a) and $\Delta = 250$ meV (b). The white areas in (a) and (b) represent insulating regions. $n^{(rms)}$ (c) and $V_{D,sc}^{(rms)}$ (d) as a function of doping for $n_{imp} = 3 \times 10^{11}$ cm^{-2} and different values of Δ, from top to bottom in (c) [bottom to top in (d)] $\Delta = 12, 23, 35, 46,$ and 55 meV. The dashed line in (c) and (d) shows the value of $n^{(rms)}$ and $V_{D,sc}^{(rms)}$, respectively, for the gapless case. The insets show the results for $\Delta = 500$ meV [29].

FIG. 2 (color online). Color plots showing A_i as a function of n_{imp} and $\langle n \rangle$ for $\Delta = 125$ meV (a), $\Delta = 250$ meV (b), and $\Delta = 500$ meV (c). (d) Δ_{cr} as a function of n_{imp} for different values of Δ. (e) Δ_{cr} as a function of Δ for different values of n_{imp}. (f) $\Delta_{cr}/(\Delta/2)$ as a function of V_D/Δ. The filled (unfilled) symbols, connected by the solid (dashed) line, show the dependence of $\Delta_{cr}/(\Delta/2)$ with respect to $V_{D,sc}^{(rms)}/\Delta$ [$(eV_D^{(rms)}/\epsilon)/\Delta$]. The different symbols, circles, squares, diamonds, and triangles, show the results for $\Delta = 500, 250, 125,$ and 62.5 meV, respectively. [29].

the contour for which the area fraction occupied by electron puddles is equal to 50%. Below this line, more than half of the sample area is occupied by hole puddles and insulating regions. Finally, the red line shows the contour for which $A_i = 0.5$. Below this line, more than half of the sample is covered by insulating regions. The counterintuitive result is that close to the CNP A_i becomes smaller as n_{imp} increases with $\langle n \rangle$ fixed. This is a consequence of the fact that as n_{imp} increases, the disorder becomes strong enough to bring the Fermi level inside the conduction or the valence band. Using the contour lines overlaid on the color plot for A_i, we can qualitatively identify different semiclassical transport regimes. Regime I: Weak disorder where $n^{(rms)} \ll \langle n \rangle$.—The system is a good metal with an almost uniform density landscape. Regime II: Strong disorder $n^{(rms)} > \langle n \rangle$.—In this regime the density landscape breaks up in puddles and insulating regions. Because the area fraction covered by electrons is larger than $1/2$, the system behaves like a metal via percolation through the electron puddles. Regime III: Weak-moderate disorder, $|\mu| < \Delta/2$, $V_{D,sc}^{(rms)} < \Delta/2$.—Most of the sample area is insulating and the system is an insulator. Regime IV.—In this regime the disorder is so strong, $V_{D,sc}^{(rms)} \gg \Delta/2 > |\mu|$, that, despite the finite gap, A_i is less than 50% but neither the electron puddles nor the hole puddles alone cover more than 50% of the total area. The system should behave as a bad metal with the conductance determined by tunneling events across a few narrow insulating regions separating the electron-hole puddles similar to transport at the CNP in gapless BLG [27] and SLG [28]. It is obvious, by looking at the color plots in Figs. 2(a)–2(c), that at lower (higher) values of Δ (disorder) the apparent transport gap will be strongly suppressed and in fact will be vanishingly small. We believe that this is the current physical situation in existing BLG systems.

To identify the transport regime, it is useful to introduce the critical value of chemical potential Δ_{cr}, for which $A_i = 50\%$. For $\mu > \Delta_{cr}$ ($\mu < \Delta_{cr}$) the system is expected to behave as a bad metal (an insulator). For $\Delta \gg V_{D,sc}^{(rms)}$, $\Delta_{cr} \approx \Delta/2$ is almost independent of the disorder strength. For small gaps, $\Delta \lesssim V_{D,sc}^{(rms)}$, Δ_{cr} depends strongly on the disorder strength, and $\Delta_{cr} \ll \Delta$. This is shown in Fig. 2(d), in which the calculated Δ_{cr} as a function of n_{imp} is shown for four different values of Δ. For fixed Δ, Δ_{cr} decreases as n_{imp} increases. We see that for $\Delta \lesssim 150$ meV, for impurity densities of the order of the ones estimated in current experiments on exfoliated BLG ($n_{imp} \approx 10^{12}$ cm^{-2}), Δ_{cr} can be orders of magnitude smaller than Δ. Figure 2(e) shows Δ_{cr} as a function of Δ for different values of n_{imp}. We see that, for $\Delta \approx 100$ meV, $\Delta_{cr} \approx 0$ already for $n_{imp} \approx 3 \times 10^{11}$ cm^{-2}. In the presence of spatial correlations among impurities, the density inhomogeneities are expected to be reduced, and therefore the value of n_{imp} for which $\Delta_{cr} \to 0$ would increase. Finally, Fig. 2(f) shows the

scaling of Δ_{cr} on the strength of the disorder potential V_D. The points connected by solid (dashed) lines show the dependence of $\Delta_{cr}/(\Delta/2)$ with respect to $V_{D,sc}^{(rms)}/\Delta$ $[(eV_D^{(rms)}/\epsilon)/\Delta]$, with $V_D^{(rms)}$ the rms of the bare disorder potential. In both cases, by normalizing both Δ_{cr} and V_D with the band gap, we find that the results obtained for different values of Δ collapse on a single curve that does not depend on Δ and away from $V_D = 0$ scales approximately as $1 - ae^{bV_D/\Delta}$, with ($a = 0.02$, $b = 1.52$) for $V_D = eV_D^{(rms)}/\epsilon$ and ($a = 0.015$, $b = 6.65$) for $V_D = V_{D,sc}^{(rms)}$.

In summary, using a simple 2-bands model and TFT, we have characterized the density inhomogeneities in gapless and gapped BLG. For gapless BLG, we have found analytic expressions for $n^{(rms)}$ and $V_{D,sc}^{(rms)}$ as a function of the experimental parameters and shown that they do not depend on the doping and scale like $\sqrt{n_{imp}} f^{1/2}(d/r_{sc})/r_{sc}$. For gapped BLG, $n^{(rms)}$ ($V_{D,sc}^{(rms)}$) is reduced (enhanced) with respect to the gapless case, in particular, in the vicinity of the CNP. By calculating the disorder-averaged fraction of the sample area A_i covered by insulating regions, we have qualitatively identified four different transport regimes. We have shown that most of the current experiments are expected to be in a regime, regime IV, in which the disorder is strong enough to reduce A_i below 50% even at zero doping. In this regime, gapped BLG is expected to behave like a bad metal in which transport is dominated by hopping processes between electron and hole puddles that cover most of the sample. The value of the chemical potential Δ_{cr} for which $A_i = 0.5$ identifies the crossover between the insulating regime and regime IV. We have shown how Δ_{cr} depends on the impurity density n_{imp}, the strength of the screened disorder potential, and the theoretical band gap Δ. We believe the reduction of Δ_{cr} as a function of n_{imp} is the qualitative resolution of the contradiction between Δ and the transport gap. A clear prediction of our theory is that in cleaner BLG (e.g., on boron-nitride substrates) there should be close agreement between the transport gap and Δ. We also predict agreement between Δ and the transport gap for very large values of Δ.

[1] K. S. Novoselov *et al.*, Science **306**, 666 (2004).
[2] S. Das Sarma *et al.*, Rev. Mod. Phys. **83**, 407 (2011).
[3] S. V. Morozov *et al.*, Phys. Rev. Lett. **100**, 016602 (2008).
[4] S. Xiao *et al.*, Phys. Rev. B **82**, 041406 (2010).

[5] E. H. Hwang, E. Rossi, and S. Das Sarma, Phys. Rev. B **80**, 235415 (2009).

[6] C. R. Dean *et al.*, Nature Nanotech. **5**, 722 (2010).

[7] S. Das Sarma and E. H. Hwang, Phys. Rev. B **83**, 121405 (R) (2011).

[8] E. V. Castro *et al.*, Phys. Rev. Lett. **99**, 216802 (2007).

[9] H. Min *et al.*, Phys. Rev. B **75**, 155115 (2007).

[10] Y. B. Zhang *et al.*, Nature (London) **459**, 820 (2009).

[11] J. Oostinga *et al.*, Nature Mater. **7**, 151 (2007).

[12] T. Taychatanapat and P. Jarillo-Herrero, Phys. Rev. Lett. **105**, 166601 (2010).

[13] K. Zou and J. Zhu, Phys. Rev. B **82**, 081407 (2010).

[14] J. Yan and M. S. Fuhrer, Nano Lett. **10**, 4521 (2010).

[15] J. Li *et al.*, Nature Phys. **7**, 38 (2011).

[16] T. O. Wehling *et al.*, Phys. Rev. Lett. **105**, 056802 (2010); A. Ferreira *et al.*, Phys. Rev. B **83**, 165402 (2011).

[17] M. I. Katsnelson and A. K. Geim, Phil. Trans. R. Soc. A **366**, 195 (2008); F. Guinea, J. Low Temp. Phys. **153**, 359 (2008).

[18] J. T. Chalker and P. D. Coddington, J. Phys. C **21**, 2665 (1988); A. L. Efros, F. G. Pikus, and V. G. Burnett, Phys. Rev. B **47**, 2233 (1993); E. Shimshoni, A. Auerbach, and A. Kapitulnik, Phys. Rev. Lett. **80**, 3352 (1998).

[19] E. Arnold, Surf. Sci. **58**, 60 (1976); A. L. Efros, Solid State Commun. **70**, 253 (1989); Y. Meir, Phys. Rev. Lett. **83**, 3506 (1999); S. Ilani *et al.*, Science **292**, 1354 (2001); J.

Shi and X. C. Xie, Phys. Rev. Lett. **88**, 086401 (2002); S. Das Sarma *et al.*, Phys. Rev. Lett. **94**, 136401 (2005); G. Allison *et al.*, Phys. Rev. Lett. **96**, 216407 (2006); M. J. Manfra *et al.*, Phys. Rev. Lett. **99**, 236402 (2007).

[20] M. Han *et al.*, Phys. Rev. Lett. **98**, 206805 (2007); M. Y. Han, J. C. Brant, and P. Kim, Phys. Rev. Lett. **104**, 056801 (2010); S. Adam *et al.*, Phys. Rev. Lett. **101**, 046404 (2008); P. Gallagher, K. Todd, and D. Goldhaber-Gordon, Phys. Rev. B **81**, 115409 (2010).

[21] E. Rossi and S. Das Sarma, Phys. Rev. Lett. **101**, 166803 (2008).

[22] M. Polini *et al.*, Phys. Rev. B **78**, 115426 (2008).

[23] J. Martin *et al.*, Nature Phys. **4**, 144 (2008).

[24] Y. Zhang *et al.*, Nature Phys. **5**, 722 (2009).

[25] A. Deshpande *et al.*, Phys. Rev. B **79**, 205411 (2009).

[26] L. Brey and H. A. Fertig, Phys. Rev. B **80**, 035406 (2009).

[27] S. Das Sarma, E. H. Hwang, and E. Rossi, Phys. Rev. B **81**, 161407 (2010); E. H. Hwang and S. Das Sarma, Phys. Rev. B **82**, 081409 (2010).

[28] E. Rossi, S. Adam, and S. Das Sarma, Phys. Rev. B **79**, 245423 (2009).

[29] Even for large electric fields in BLG, Δ saturates to ~ 250 meV. Results for $\Delta > 250$ meV are shown to illustrate qualitatively the situation $\Delta \gg V_{D,\mathrm{sc}}^{(\mathrm{rms})}$ typical in standard parabolic 2DEGs such as the ones created in GaAs and Si quantum wells.